PAPER

On the electronic specific heat of liquid tungsten

IOP Publishing Journal of Physics: Condensed Matter
J. Phys.: Condens. Matter **26** (2014) 045701 (7pp) doi:10.1088/0953-8984/26/4/045701

On the electronic specific heat of liquid tungsten

V N Korobenko and A D Rakhel

Joint Institute for High Temperatures, Izhorskaya 13, Building 2, Moscow 125412, Russia

E-mail: rakhel@oivtran.ru

Received 28 August 2013, revised 31 October 2013
Accepted for publication 20 November 2013
Published 6 January 2014

Abstract

Tungsten foil strip sandwiched between two sapphire plates was rapidly heated by an electrical current pulse so that it experienced a two-fold thermal expansion in less than 400 ns under increasing dynamic pressure. The dependence of density on specific enthalpy and pressure was investigated for liquid tungsten using two essentially different diagnostic techniques. Based on a comparison of the results with each other and literature data the systematic uncertainty of the measurements has been estimated. The dependence of density on specific enthalpy along the isobar $P = 0.1$ MPa has been determined for the entire liquid range. The data have been used to evaluate the constant volume specific heat of liquid tungsten and the electronic contribution to it. It has been shown that the contribution attains more than 40% of the total value of the specific heat.

Keywords: thermal expansion, electronic specific heat, liquid tungsten

(Some figures may appear in colour only in the online journal)

1. Introduction

The thermal expansion of liquid tungsten has been measured by a number of authors. However, scattering among the most accurate data on the density of the liquid near the normal melting point exceeds 7%, so that uncertainty in the thermal expansion coefficient is about 100% [1]. For condensed matter physics, the thermal expansion coefficient is of special interest because this quantity relates the usually measured specific heat at constant pressure C_P to the specific heat at constant volume C_V which is used for the evaluation of the electronic contribution to the thermodynamic functions. Accurate data on the electronic specific heat are needed to construct the interatomic potentials used in large-scale atomistic simulations [2, 3], to model the processes induced in the target metals by the femtosecond lasers [4], and to investigate the metal-to-nonmetal transition phenomenon in expanded liquid metals [5].

For the specific heat C_V of liquid tungsten the experimental data [6] provide values which are very close to the classical Dulong–Petit's value $3R$ (R is the gas constant). This means that the electronic contribution to the specific heat is negligible. On the other hand, the unexpectedly high critical pressure of tungsten ($P_c > 7$ GPa) and the enthalpy values in the two-phase state, which are three times the heat of sublimation at room temperature [7], indicate that the electronic contribution to the thermodynamic functions is crucial. Thus, an accurate estimate of the electronic contribution to the specific heat deserves close attention.

The standard thermodynamic relation between the specific heats reads

$$C_V = \frac{C_P^2}{C_P + A\alpha^2 c_S^2 T} \tag{1}$$

where A is the atomic weight, T is the temperature, c_S is the velocity of sound and α is the thermal expansion coefficient

$$\alpha = \frac{1}{V}\left(\frac{\partial V}{\partial T}\right)_P \tag{2}$$

(C_P and C_V are given per mol). Hence, to get precise data on C_V we need to measure accurately not only the specific heat C_P but also the velocity of sound c_S and the thermal expansion coefficient α. As will be shown in section 5, whilst the specific heat C_P and the velocity of sound of liquid tungsten have been measured with a sufficient accuracy, the values of the

thermal expansion coefficient, measured solely by means of the exploding wire technique, are very uncertain. This work provides a value of α which is accurate to $\pm 15\%$, so that the constant volume specific heat and the electronic contribution to it can be determined with a precision better than $\pm 30\%$.

Our measurements have been done mainly by means of the fast dynamic technique [8, 9]. To estimate the systematic uncertainty of the measurements we have developed an alternative experimental technique. This paper presents the measurement results on the density of liquid tungsten as a function of specific enthalpy and pressure obtained by the both techniques. Unlike [7], we are focused here on an accurate determination of the dependence of density on specific enthalpy along the isobar $P = 0.1$ MPa. Based on the results, and using the literature data on C_P, we have determined the thermal expansion coefficient of liquid tungsten for the normal pressure isobar, which turned out to be about two times smaller than the value of [6]. The here-determined value of α along with the literature data on the sound velocity c_S and C_P have been used to determine the constant volume specific heat C_V and the electronic contribution to it. We show that the contribution approaches the value $3R$, a result that agrees with the theoretical estimates based on the density functional theory computations of the electron density of states [4, 10].

2. Measurement method

Tungsten foil strip of 20 μm thickness and 6 mm width is sandwiched between two flat sapphire plates with the face surfaces polished to optical quality. The experimental assembly is carefully glued by UV-curing adhesive so that the gaps between the elements of the assembly are entirely filled with the glue and the thicknesses of the layers of the glue between the sample and the sapphire plates are less than 3 μm. A photo of such an experimental assembly is shown in figure 1. In the experiment the sample is heated by an electrical current pulse produced by discharging a high-power capacitor bank. As was shown in the previous works [8, 9], the technique ensures a sufficiently homogeneous and practically one-dimensional thermal expansion of the sample (in the direction perpendicular to the foil strip surface) during the time interval $t < 1$ μs. The primary measured quantities in the experiments are the electric current I through the sample, the voltage drop U across it, and the pressure P near the sample. The last quantity is measured using the ruby pressure scale (RPS) technique [11]. The thermal expansion of the sample volume is determined from the measured time dependence of the pressure using the Poisson adiabatic equation of sapphire [8]. To perform the pressure measurements a ruby plate is placed between the sample and one of the sapphire plates (see figure 1). The R-lines luminescence is excited in the ruby plate by a pulsed laser and is detected by means of a streak camera and a spectrograph. In each experiment, from the measured quantities, we get the time dependence of the specific enthalpy $W(t)$, the specific volume $V(t)$, the pressure $P(t)$, and the electric conductivity $\sigma(t)$. By eliminating time we obtain the dependence $W(P, V)$ and $\sigma(P, V)$ along a line on the PV-plane which represents the thermodynamic path of

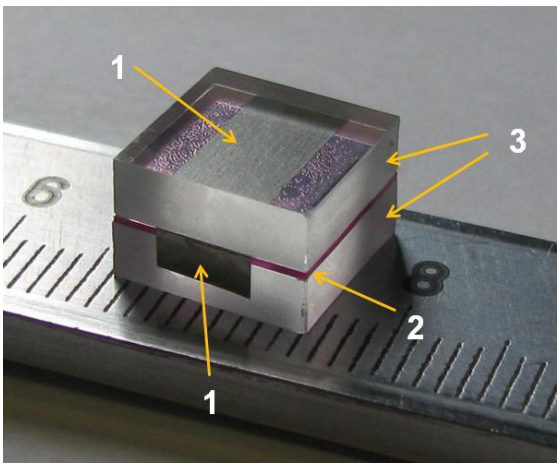

Figure 1. Photograph of the experimental assembly: a tungsten foil strip (1) together with ruby plate (2) is sandwiched between two sapphire plates (3). In the experiment the bent ends of the foil strip (one of the ends is visible in the photograph) are pressed to the electrodes delivering the heating current pulse to the sample.

the experiment. In order to obtain the functional relationships $W(P, V)$ and $\sigma(P, V)$ for a certain region of the PV-plane we conduct a series of experiments, the thermodynamic paths of which pass through the region. Values of the pressure, density, enthalpy, and conductivity can be measured with an accuracy better than $\pm 10\%$ [7, 9].

To estimate the systematic uncertainty of the measurements we have developed an alternative experimental technique which allows the displacement of the sample–sapphire interface to be detected directly. The technique is based on the use of an interferometer and its essence is as follows. On the free surface of the front sapphire plate of the experimental assembly shown in figure 1 (but without the ruby plate) a laser ray with wavelength $\lambda_0 = 1.550$ μm (in air) is incident normally. The ray is partially reflected from the free surface of the plate, and partially refracted into it and then reflected from the sample surface. The two rays are superimposed on each other and the light intensity in the region of interference is recorded with a fast photodetector and an oscilloscope. When the sample surface is displaced due to thermal expansion, the difference between the optical paths of the interfering rays is changed, which causes oscillations in the light intensity on the photodetector. For more details see [7].

The displacement of the sample surface caused by the thermal expansion can be determined from the measured time dependence of the light intensity of the interfering rays. Due to the linear dependence of the refractive index of sapphire on density [12], the displacement can be determined directly without measuring the deformation of the sapphire plates. The relation between the time dependence of the light intensity and the change in the sample thickness is derived in the appendix. Figure 2 shows the photodetector signal for an experiment with a tungsten sample in the form of a foil strip placed between two sapphire plates and heated by an electrical current pulse. The initial thickness of the foil strip was 22 μm, the width was 5 mm, and the length was 10 mm.

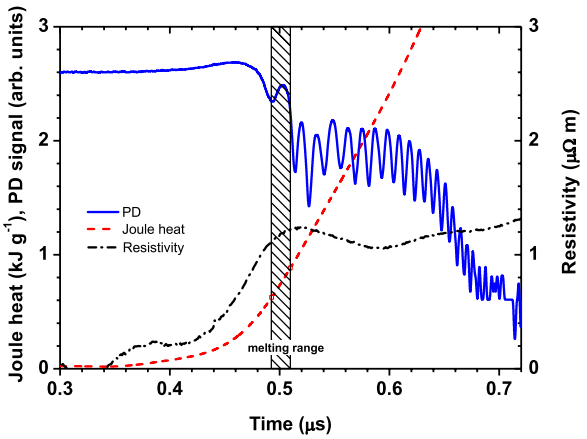

Figure 2. Time dependences of the photodetector (PD) signal (thick blue line), the Joule heat dissipated in the tungsten sample (red dashed line), and the resistivity related to the initial cross sectional area of the sample (black dash–dot line).

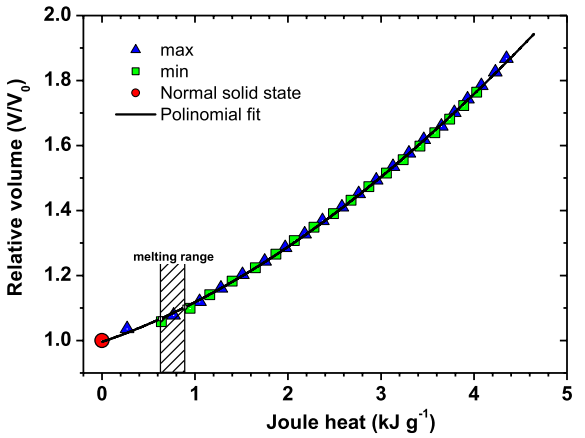

Figure 3. The relative volume as a function of the Joule heat dissipated in the sample (per unit mass). The values of the relative volume were determined by formula (A.7) and correspond to the instants at which the photodetector signal has maxima (blue triangles) and minima (green squares). The black line shows the polynomial fit used to calculate the pressure.

The sapphire plates had a thickness of 5 mm and both a width and length of 10 mm. As follows from this figure, the positions of the extrema in the signal are well resolved up to the time $t = 0.68$ μs.

Figure 3 shows the relative volume V/V_0 determined by equation (A.7) from the photodetector signal presented in figure 2 at the instants corresponding to the maxima and minima in the signal as a function of the Joule heat dissipated per unit mass of the sample. Here $V_0 = 0.0518$ cm^3 g^{-1} is the specific volume of tungsten in the normal solid state.

After measuring the sample volume by the interferometric technique we can determine the pressure. As the sapphire plates start to move from a state of rest and the movement is isentropic, it is described by the simple wave solution [13]. In such a wave the pressure exerted on the sample–sapphire interface can be expressed in terms of the interface velocity $U(t)$:

$$P(t) = \frac{B}{n}\left[\left(\frac{n-1}{2c_0}U(t)+1\right)^{2n/(n-1)} - 1\right], \qquad (3)$$

where $B = 499.0$ GPa, $n = 3.0$, and $c_0 = \sqrt{B/\rho_0}$ is the velocity of sound in sapphire [8]. Thus, by differentiating the measured time dependence of the displacement of the sample–sapphire interface, we determine the velocity $U(t)$, then the pressure is calculated by equation (1).

We present here results of six experiments. In four experiments of this series we used the RPS technique. In these experiments the geometrical dimensions of the samples and the sapphire plates were identical. The samples were cut from a tungsten foil of 20 μm nominal thickness and 99.95% nominal purity (with the content of Mo not more than 0.023% by mass) in the form of strips of 6 mm width and 10 mm length (measured with an error less than 0.1 mm). The actual thickness of the samples was determined with an error less than 0.4 μm from the known density of the foil, $V_0^{-1} = 19.3 \pm 0.1$ g cm^{-3}, by weighing the samples with an uncertainty less than 2×10^{-6} g. The surface of the foil had a metallic luster and the roughness was less than 1 μm. The ruby plates were c-cut plates with a 0.28% concentration of Cr by weight, of 400–420 μm thickness, and 10 mm width and length. The sapphire plates had a 3 mm thickness, and were 10 mm both in width and length. On the side of the ruby plate facing the sample, a multilayer dielectric mirror of thickness 2 μm was deposited. This mirror reflected the laser light pumping the luminescence and made the pumping more effective. In the other two experiments of this series, the thermal expansion of the samples was measured by the interferometric technique.

The samples in the experiments were rapidly heated by electrical current pulses from discharges of a capacitor bank. The current through the sample was measured with a Rogowski coil and the voltage between the electrodes at the ends of the sample was measured by a voltage divider. The resistance and the Joule heat dissipated in the sample were calculated by the well-known formulas. The determination of the specific enthalpy and conductivity from the measurement results is straightforward [8].

3. Results of the measurements

Figure 4 shows results of the measurements of the density of solid and liquid tungsten as a function of specific enthalpy. The results of the interferometric measurements are compared with those obtained by the RPS technique. From figure 4 it follows that for fixed values of the enthalpy the differences between the density values measured here by the two techniques do not exceed 3%. As can be also seen from this figure, our results are in good agreement (the difference is less than 3%) with the data of the measurements [14–17] having an uncertainty <2%. The literature data in the original works are presented as dependences of the specific volume versus temperature. To determine the enthalpy values for those data we used the recommended value for solid tungsten of the

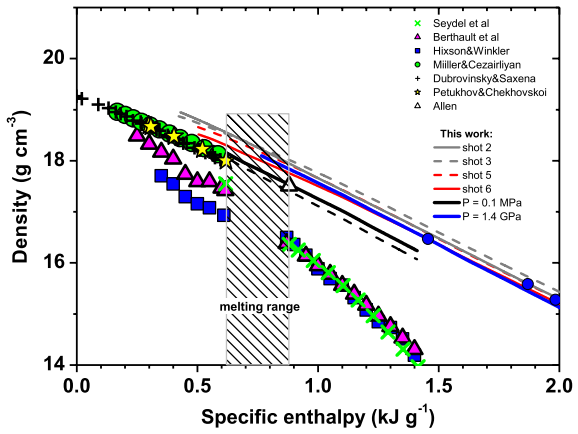

Figure 4. Density of solid and liquid tungsten as a function of specific enthalpy. The density measured in this work by the interferometric technique (red lines) is compared with the results obtained by the RPS technique (gray lines). The isobars $P = 0.1$ MPa and $P = 1.4$ GPa determined from the data in this work and using the literature data on the sound velocity are shown by the black lines and the blue line respectively (see text). The three values of density directly measured in this work on the isobar $P = 1.4$ GPa are shown as blue circles.

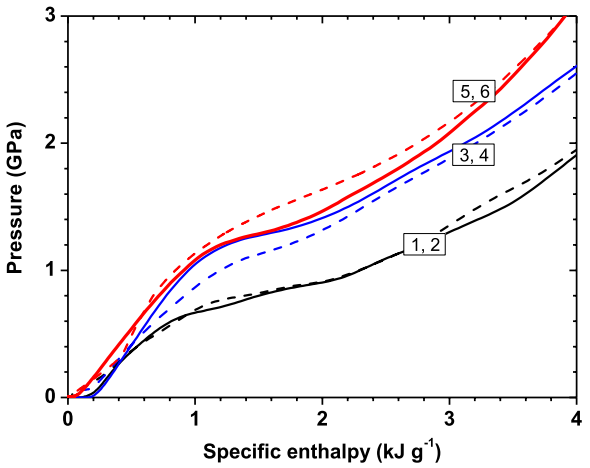

Figure 5. Pressure as a function of specific enthalpy for the experiments in this work. In experiments 1–4 the pressure was measured by the RPS technique, whilst in experiments 5 and 6 the interferometric technique was used. For each pair of experiments the parameters controlled were identical.

dependence of the temperature on the enthalpy from [18]. Based on the comparison shown in figure 4, we estimated the accuracy of the present interferometric measurements of density to be better than 5% and that of the RPS technique to be better than 6%. As seen from figure 4, the data of [6, 19–21] differ significantly from our results. On the other hand, there is a good agreement between our results and the results in [22, 23]. In the last work the density was measured using the capillary tubes technique (those results are not shown in figure 4 because of their large scatter).

The pressure as a function of specific enthalpy for the experiments in this work is presented in figure 5. As seen from the figure, in the enthalpy range from 0.9 to 1.4 kJ g^{-1} the pressure increases from about 0.5 to 1.5 GPa. To compare accurately our results with the literature data measured at atmospheric pressure [16, 17] or at the static pressures 0.3 GPa [6] and 0.2 GPa [19], we have determined from our data the dependence of the density versus the specific enthalpy along the isobars $P = 0.1$ MPa and $P = 1.4$ GPa. This was done as follows. Since at pressures in the range 0.5–1.5 GPa the compressibility of liquid tungsten is relatively small, we can expand the density ρ in powers of the pressure change $P - P_0$ near an isobar $P = P_0$ and drop all terms except the linear one. Hence we get the formula

$$\rho(W, P_0) \approx \rho(W, P) - \left(\frac{\partial \rho}{\partial P}\right)_W (P - P_0) \qquad (4)$$

where W is the specific enthalpy. For the derivative in the right-hand side of equation (4) the following relation holds

$$\left(\frac{\partial \rho}{\partial P}\right)_W = \beta + c_S^{-2} \qquad (5)$$

where

$$\beta = \frac{1}{V}\left(\frac{\partial V}{\partial W}\right)_P. \qquad (6)$$

The last derivative can be related to the thermal expansion coefficient: $\beta = \alpha A / C_P$. Using values of β and c_S measured in [6, 14–19] , and the dependences $\rho(W, P)$ measured here along the paths in the WP-plane shown in figure 5, we found by equation (2) the dependence $\rho(W, P_0)$ along the isobar $P = 0.1$ MPa. In figure 4 the dependence is shown as the black dashed line. As seen from this figure, this dependence differs only slightly from the dependences $\rho(W, P)$ measured along the paths with rising pressure. On the other hand, the value of β determined from this dependence is about two times smaller than that of the data in [6, 19]. Hence we can obtain a more precise dependence $\rho(W, P_0)$ if we use the here-determined value of the derivative β. The corresponding dependence of the density versus the specific enthalpy along the isobar $P = 0.1$ MPa is shown in figure 4 as the thick black line. We have also determined the dependence of the density along the isobar $P = 1.4$ GPa and compared it with several values of the density directly measured at this pressure in our experiments. As one can see from figure 4, the isobar determined by equation (2) agrees well with the directly measured values. A linear fit of the determined dependence of the density versus the specific enthalpy on the isobar $P = 0.1$ MPa is given by

$$\rho = 19.67 - 2.43W, \qquad (7)$$

where the density ρ is measured in g cm^{-3} and the specific enthalpy W in kJ g^{-1}.

4. Discussion of the measurement errors

As seen from figure 2, our measurements were performed during less than 0.3 μs, which is about two orders of magnitude shorter than in the experiments [6, 19, 20]. Therefore, for an accurate determination of the heat dissipated in the sample, special attention should be paid to the determination of the inductive part of the voltage drop

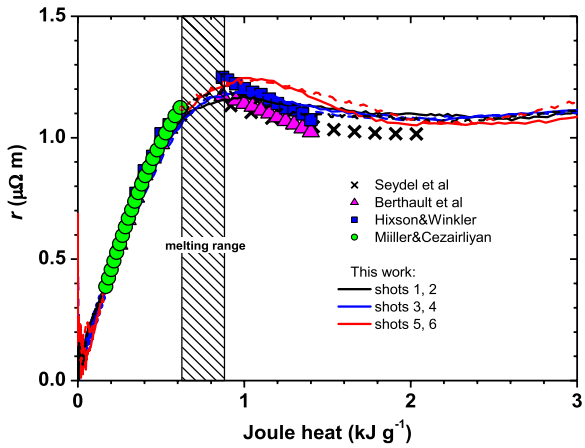

Figure 6. The resistivity related to the initial cross sectional area of the sample as a function of the heat dissipated in it. Our results are shown as lines and the marks represent the results of [6, 15, 16, 19, 20].

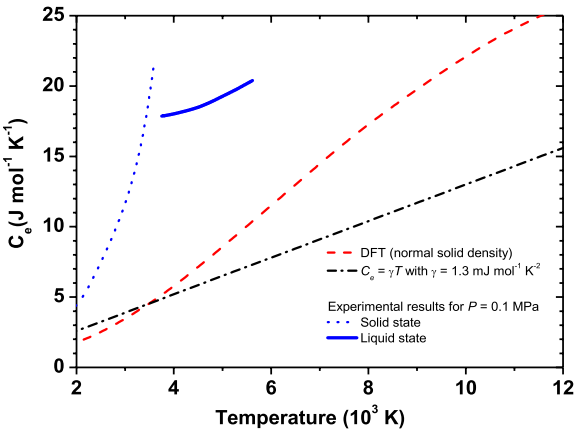

Figure 7. Molar electronic specific heat of tungsten C_e determined for the solid (blue dotted line) and liquid state (blue thick line) on the isobar $P = 0.1$ MPa is compared with the results of DFT calculations of [4] (red dashed line) and the extrapolation of the low temperature dependence with the value of γ taken from [29] (black dot dashed line); the normal melting and boiling point temperatures of tungsten are $T_m = 3.69 \times 10^3$ K and $T_b = 5.645 \times 10^3$ K, respectively [30].

across the sample. In our experiments the foil strips had thicknesses much smaller than their width and length, so that the inductance remained practically constant. This is evident from the formula for the inductance of the foil strip [24]

$$L = 2l\left[\ln\left(\frac{2l}{d+h}\right) + 0.5\right], \tag{8}$$

where l is the length of the strip, h is the width and d is the thickness. In equation (8) the inductance is measured in nH and the geometric dimensions are in cm. Since during the experiments the inductance practically does not change and the geometric dimensions of the samples were almost equal to each other, the value of the inductance could be determined sufficiently accurately. To verify that the inductance has been determined with sufficient accuracy, we show in figure 6 the dependence of the so-called resistivity related to the initial cross sectional area of the sample r versus the heat dissipated in it. This quantity

$$r = R_S S_0 / l, \tag{9}$$

where R_S is the resistance of the sample and S_0 is its initial cross sectional area, by virtue of the homogeneous and 1D thermal expansion ($l = \text{const}$ and $h = \text{const}$), and due to the conservation of mass, so that the current cross sectional area $S = S_0\rho_0/\rho$, is related to the conductivity and density by the formula

$$r = \frac{V_0}{V}\sigma^{-1}. \tag{10}$$

Thus, r is directly related to the properties of the material and do not depend on the geometric dimensions of the sample. On the other hand, to determine this quantity we do not need to know the thermal expansion of the sample, whose uncertainty is essentially larger than that of the electrical quantities. As seen from figure 6, in the solid state range, for which we can neglect the difference between the pressure in our experiments and in the experiments at atmospheric pressure, our measurements are in very good agreement with the results of [6, 15, 16, 19, 20].

Estimates of errors in the measured and here-computed quantities give the following uncertainties in the values of the properties. Uncertainties in the specific enthalpy measurements are less than 7%. Uncertainty in the density measured by the interferometer is less than 5% and that by the PRS technique is less than 6%. Uncertainty of the pressure measurements by the interferometer is about 0.45 GPa for the enthalpy values above 1 kJ g^{-1}. The pressure measurements using the RPS have an uncertainty of 0.2 GPa over the entire enthalpy range.

5. The electronic contribution to the constant volume specific heat

We calculated the specific heat C_V using equation (1). The value of β has been determined from the present work using the isobar $P = 0.1$ MPa, shown in figure 4 as the thick black line. The other quantities which appear in equation (1) were taken from the literature. The specific heat C_P of liquid tungsten has been measured by many authors using different methods and the scatter between the most accurate data is less than 7%. In the calculations we used the value $C_P = 51.5$ J mol^{-1} K^{-1} from [25]. The data on the velocity of sound were taken from [6]. The last data were corrected with respect to the density values (the correction is less than 7%). For the solid state range the temperature T was determined from the dependence of the specific enthalpy on temperature recommended in [18]. Since the anharmonic contribution to C_V is small [26], the electronic term C_e was evaluated by subtracting from C_V Dulong and Petit's value of $3R$, which gives the maximum contribution of atoms. The difference $C_e = C_V - 3R$ determined for the solid and the entire range of the liquid state along the isobar $P = 0.1$ MPa

is presented in figure 7. As one can see, C_e increases with temperature, as it should be, and its magnitude is less than the maximal value predicted by the DFT calculations for the normal solid density [4]. The difference $C_V - 3R$ increases remarkably already in the solid state so that its values near the melting point become comparable with those in the liquid state. Since the high level of the difference in the solid state cannot be ascribed to the effects of anharmonicity or vacancy formation [26, 27] we conclude that it is due to the electronic contribution. Therefore, the relatively large value of the constant pressure specific heat of liquid tungsten, $C_P \approx 6.2R$, is due to the electronic contribution. This result is very similar to that obtained for molybdenum [10]. The existence of the electronic contribution to C_V, which is comparable to Dulong and Petit's value, agrees with the results of [7], where unexpectedly large enthalpy values have been measured in liquid tungsten. It should be noted that over the entire liquid state density range corresponding to the isobar $P = 0.1$ MPa, tungsten remains in the metallic state [7].

Acknowledgments

We wish to express our gratitude to Mr Pierre Noiret for his valuable discussion on the subject of the paper and assistance in preparation of the poster for the presentation at the 10th International Workshop on Subsecond Thermophysics [28]. This work was partially supported by the Presidium of the Russian Academy of Sciences in the framework of the Program P-02 'Matter under extreme conditions'.

Appendix

Let us show how the time dependence of the light intensity in the region of interference of the rays is related to the thermal expansion of the tungsten foil strip sandwiched between two sapphire plates. Figure A.1 shows a schematic diagram of the concept. A laser ray of fixed wavelength and linear polarization state (1) is incident normally on the free surface of the sapphire plate. It is partly reflected from the surface (2), and partly refracted into it and then reflected from the sample (3). Using a fast photodetector we record the oscillations of the light intensity in the region of interference of the rays 2 and 3.

We shall assume that direction of polarization of the plane-polarized light does not change during the reflections and refractions. As is well known, the interference term in the intensity depends on the difference in the optical paths of the rays. Let us calculate the difference between the optical paths of rays 2 and 3 at the position $x = X_2$, assuming for simplicity that the interference is observed at the surface of the sapphire plate. Let the phase of the incident ray 1 at the instant $t = 0$ and at the point $x = X_2$ be zero. Then the phase of ray 2 at the same point at an instant $t = \tau$ is $\phi_2 = \Delta\phi_2 + \omega_0\tau$, where ω_0 is the angular frequency of the incident ray and $\Delta\phi_2$ is a phase jump caused by the reflection from the free surface of sapphire. Let τ be the interval of time during which the constant phase point on the wave profile of ray 3, which

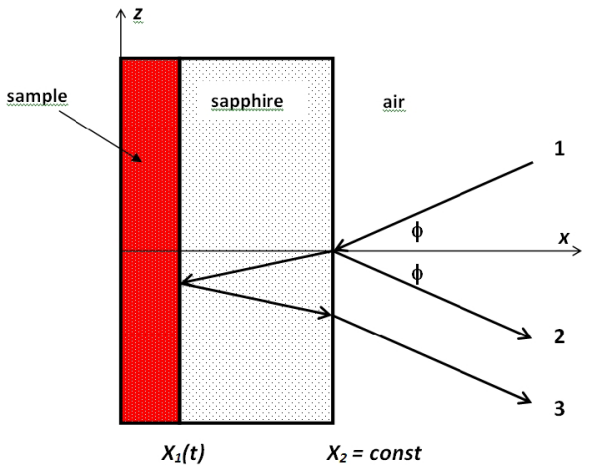

Figure A.1. Diagram illustrating the concept of the interferometric measurements. Interference is obtained when the laser ray reflected from the free surface of the front sapphire plate (2) is superimposed on the ray reflected from the sample (3). In our experiments the ray (1) is incident normally on the sapphire plate, but in this figure for clarity of the representation the angle ϕ is taken as non-zero. The figure shows only half of the assembly on the right of the plane of symmetry $x = 0$.

propagates with the phase velocity, traverses the path from the free surface to the sample surface and then back in the reverse direction. Then the phase of ray 3 at $x = X_2$ and for $t = \tau$ is equal to the sum of the phase jumps $\Delta\phi_3$ caused by the refraction of ray 3 from air into sapphire, the reflection from the sample surface and the refraction from sapphire into air. Hence the required phase difference is

$$\phi_3 - \phi_2 = \Delta\phi_3 - \Delta\phi_2 - \omega_0\tau. \tag{A.1}$$

To determine the difference we need to calculate τ. In a homogeneous medium the point of the wave profile corresponding to a fixed phase propagates with the velocity $u = c/n_r$, where c is the light velocity in vacuum and n_r is the refractive index of the medium. For an inhomogeneous medium, when the spatial scale of the inhomogeneity is larger than the wavelength of the light, in a small distance dx near the point x the wave traverses with a velocity which corresponds to the local value of the refractive index $n_r(x)$. Hence the fixed phase point traverses the path from the free surface of the sapphire plate to the sample surface during the time

$$\tau_1 = -\frac{1}{c}\int_{X_2}^{X_1(t)} n_r\,dx, \tag{A.2}$$

where $X_1(t)$ and X_2 are the coordinates of the sample surface and the free surface of the sapphire plate, respectively (see figure A.1). It can be easily shown that for velocities $dX_1/dt \leq 100$ m s^{-1}, which are typical for our experiments, we can neglect the displacement of the sample surface during the time τ_1. Moreover, we can also neglect the Doppler effect due to which the frequency of the reflected ray is increased by $\Delta\omega = (2\omega_0/c)\,dX_1/dt$. Here we shall not give the simple estimates supporting the conclusion. As a result, the interval of time during which the wave returns back from the sample

surface to the sapphire free surface is $\tau_2 = \tau_1$. Therefore, for the sought phase difference we obtain the formula

$$\phi_3 - \phi_2 = \Delta\phi_3 - \Delta\phi_2 - \frac{2\omega_0}{c}\int_{X_1(t)}^{X_2} n_r \, dx. \qquad (A.3)$$

Let the phase jumps $\Delta\phi_2$, $\Delta\phi_3$ and the coordinate X_2 remain constant. The last condition is ensured by the appropriate thickness of the sapphire plate: for the time of the measurements the acoustic disturbance caused by the sample does not reach the free surface. Substituting in equation (A.3) the linear dependence of the refractive index of sapphire on density

$$n_r = a + b\rho \qquad (A.4)$$

where the parameters $a = 1.7285$, $b = 0.0044$ (for $\lambda_0 = 1550$ nm) [12], we get the following expression for the integral on the right-hand side of equation (A.3):

$$\int_{X_1(t)}^{X_2} n_r \, dx = a[X_2 - X_1(t)] + b\int_{X_1(t)}^{X_2} \rho \, dx. \qquad (A.5)$$

The integral on the right is the mass of the sapphire plate per unit surface area and therefore is a constant. If we observe the interference by measuring the instants t_m, at which the intensity has maximums ($m = 1, 2, 3$ and so on), so that during the interval of time between the m and $m + 1$ maximum then the difference ϕ_3–ϕ_2 is decreased by 2π. On the other hand, this difference can be determined from equations (A.3) and (A.5). Equating these expressions, we obtain

$$X_1(t_{m+1}) - X_1(t_m) = \frac{\lambda_0}{2a}. \qquad (A.6)$$

Since the sample is placed between sapphire plates of equal thickness, both sample–sapphire boundaries are displaced by the same distance. Therefore, the relative volume increases during this interval of time by

$$\frac{V(t_{m+1}) - V(t_m)}{V_0} = \frac{\lambda_0}{ad_0}, \qquad (A.7)$$

where d_0 is the initial thickness of the sample and V_0 is the initial specific volume of the sample material. Thus, the interferometric measurements provide a set of values $V(t_m)/V_0$ for the instants t_m, which correspond to the maximums (or/and minimums) of the light intensity in the region of interference of the rays.

References

[1] Rakhel A D, Kloss A and Hess H 2002 *Int. J. Thermophys.* **23** 1369
[2] Khakshouri S, Alfè D and Duffy D M 2008 *Phys. Rev.* B **78** 224304
[3] Belashchenko D K 2013 *Russ. J. Phys. Chem.* **87** 615
[4] Lin Z, Zhigilei L V and Celli V 2008 *Phys. Rev.* B **77** 075133
[5] Mott N 1984 *Rep. Prog. Phys.* **47** 909
[6] Hixson R S and Winkler M A 1990 *Int. J. Thermophys.* **11** 709
[7] Korobenko V N and Rakhel A D 2013 *Phys. Rev.* B **88** 13420
[8] Korobenko V N and Rakhel A D 2007 *Phys. Rev.* B **75** 064208
[9] Korobenko V N and Rakhel A D 2012 *Phys. Rev.* B **85** 014208
[10] Moriarty J A 1994 *Phys. Rev.* B **49** 12431
[11] Shen X A and Gupta Y M 1993 *Phys. Rev.* B **48** 2929
[12] Jensen B J, Holtkamp D B, Rigg P A and Dolan D H 2007 *J. Appl. Phys.* **101** 013523
[13] Landau L D and Lifshitz E M 1992 *Fluid Mechanics* (Oxford: Pergamon)
[14] Petukhov V A and Chekhovskoi V Y 1972 *High Temp.—High Press.* **4** 671
[15] Miiller P and Cezairliyan A 1990 *Int. J. Thermophys.* **11** 619
[16] Cezairliyan A and McClure J L 1971 *J. Res. Natl Bur. Stand.* **75A** 283
[17] Dubrovinsky L S and Saxena S K 1997 *Phys. Chem. Mineral.* **24** 547
[18] Gustafson P 1985 *Int. J. Thermophys.* **6** 395
[19] Berthault A, Arles L and Matricon J 1986 *Int. J. Thermophys.* **7** 167
[20] Seydel U, Fucke W and Wadle H 1980 *Bestimmung Thermophysikalischer Daten flussiger Hochschmelzender Metalle Mit Schnellen Pulsaufheizexperimenten* (Dusseldorf: Verlag P Mannhold)
[21] Kaschnitz E, Pottlacher G and Windholz L 1990 *High Press. Res.* **4** 558
[22] Allen B C 1963 *Trans. Metall. Soc. AIME* **227** 1183
[23] Ivanov V V, Lebedev S V and Savvatimskii A I 1984 *J. Phys. F: Met. Phys.* **14** 1641
[24] Kalantarov P L and Tseitlin L A 1986 *Calculation of Inductances* (Leningrad: Energoatomizdat) (in Russian)
[25] Korobenko V N and Savvatimskiy A I 2003 *AIP Conf. Proc.* **684** 783
[26] Chisolm E D, Crockett S D and Wallace D C 2003 *Phys. Rev.* B **68** 104103
[27] Grimvall G, Thiessen M and Guillermet A F 1987 *Phys. Rev.* B **36** 7816
[28] Korobenko V N and Rakhel A D 2013 *Book of Abstracts of the 10th Int. Workshop on Subsecond Thermophysics (Karlsruhe, June 2013)* p 44
[29] Kittel C 1986 *Introduction to Solid State Physics* 6th edn (New York: Wiley)
[30] Kikoin I K (ed) 1976 *Tables of Physical Quantities* (Moscow: Atomizdat) p 178 (in Russian)